

X.

GPO PRICE \$ _____

CFSTI PRICE(S) \$ _____

SCIENTIFIC NOTE

ESRO SN-4

April 1966

Hard copy (HC) 3.00

Microfiche (MF) 50

ff 853 July 65



ESRO

EXCHANGE DOCUMENT			
26	27	29	31
4	37	ESR	

INFLUENCE OF COMPRESSIBILITY ON CONDUCTION-TYPE a.c. MHD GENERATORS

by P. Ponthus

Massachusetts Institute of Technology

Cambridge, Mass., U.S.A.

N66 30871
(ACCESSION NUMBER)

53
(PAGES)

CR-76376
(NASA CR OR TMX OR AD NUMBER)

(THRU) _____

3
(CODE)

25
(CATEGORY)

**ORGANISATION EUROPÉENNE DE RECHERCHES SPATIALES
EUROPEAN SPACE RESEARCH ORGANISATION**

ESRO SN-4

April 1966

**INFLUENCE OF COMPRESSIBILITY
ON CONDUCTION-TYPE a.c. MHD
GENERATORS**

by P. Ponthus

Massachusetts Institute of Technology

Cambridge, Mass., U.S.A.

ORGANISATION EUROPÉENNE DE RECHERCHES SPATIALES

EUROPEAN SPACE RESEARCH ORGANISATION

36, rue Lapérouse, 75 - PARIS 16^e (France)

ESRO Scientific and Technical Notes are informal documents reporting on scientific or technical work carried out by the Organisation or on its behalf. The opinions presented or the conclusions reached are those of the author and do not necessarily reflect the policy of the Organisation.

ACKNOWLEDGEMENTS

The author owes the stimulus for the present study to Professor H.H. Woodson, of M.I.T., whose dynamic insights and helpful criticisms contributed greatly to the final results of this thesis.

He gratefully acknowledges the support of the European Space Research Organisation and of the National Aeronautics and Space Administration for the duration of these studies at the Massachusetts Institute of Technology.

TABLE OF CONTENTS

ACKNOWLEDGEMENTS	3
TABLE OF CONTENTS	4
TABLE OF SYMBOLS USED	6
ABSTRACT	7
SECTION I. INTRODUCTION	9
I.1 Brief History	9
I.2 The Object and Scope of This Thesis	9
SECTION II. MHD EQUATIONS IN A QUASI ONE-DIMENSIONAL ANALYSIS	11
II.1 The Equations of Conservation	11
II.2 The General MHD Equation	12
SECTION III. TIME AVERAGE EQUATIONS - DESIGN OF A COMPRESSIBLE FLUID CHANNEL WITH CONSTANT VELOCITY AND CONSTANT LOADING FACTOR. 13	13
III.1 Shape of the Channel of a d.c. Self-Excited Generator	13
SECTION IVa. PERTURBATION EQUATIONS - SMALL AMPLITUDE ANALYSIS	16
SECTION IVb. INTEGRATION OF THE VELOCITY PERTURBATION EQUATION IN SOME PARTICULAR CASES	21
IVb.1 The Velocity Perturbation Equation	21
IVb.1.1 Large Frequency	25
IVb.1.2 Zero-Order Approximation	26
IVb.1.3 General Case	27

SECTION V. VALIDITY OF THE SMALL-AMPLITUDE ANALYSIS IN THE ZERO-ORDER APPROXIMATION 28

SECTION VI. THE PROBLEM OF THE ELECTRICAL OUTPUT POWER 30

SECTION VII. CONCLUDING REMARKS 33

APPENDIX 35

REFERENCES 36

TABLE OF FIGURES 37

FIGURES 39

TABLE OF SYMBOLS USED

QUANTITY	SYMBOL	UNIT IN MKSA
<u>Geometry</u>		
distance between electrodes	w	metre
inter-pole distance	d	metre
length	ρ	metre
<u>Thermodynamics</u>		
Total pressure	P_t	Pascal or Newton/m ²
Pressure	P	
Total temperature	T_t	
Temperature	T	° Kelvin
velocity	u	metre/sec
Total enthalpy	H	
Enthalpy	h	kcal/mole kg
Entropy	S	kcal/°K-mole kg
<u>Electrical</u>		
current	I	ampere
current density	J	ampere/square metre
resistance	R	ohm
conductivity	σ	mho/metre
electric potential	V	volt
electric field intensity	E	volt/metre
magnetic flux density	B	weber/square metre or Tesla
magnetomotive force	F	ampere-turn/metre

We use subscript 0 for time-average quantities and subscript 1 for time-varying quantities. Subscript i is for "inlet".

INFLUENCE OF COMPRESSIBILITY
ON CONDUCTION-TYPE a.c. MHD GENERATOR

by

Pierre Ponthus

Submitted to the Department of Electrical Engineering
of the Massachusetts Institute of Technology
on May 21, 1965, in partial fulfillment
of the requirements for the degree of
Master of Science.

ABSTRACT

Previous analyses of configurations for generating a.c. power with MHD conduction machines that require no external reactive power supplies have been based on an incompressible fluid model. In generators using ionized gases with high power density, compressibility will cause appreciable effects. A study is made of the influence of compressibility on conduction-type MHD a.c. generators.

General MHD equations for an a.c. compressible fluid model are stated in the quasi one-dimensional analysis. Equations for perturbations which occur in an a.c. compressible fluid model are developed with the aid of a quasi one-dimensional small amplitude analysis and a numerical calculation of the perturbation velocity is performed.

The results are presented in the form of relative perturbations of velocity for various values of the appropriate parameters. The validity of the small amplitude analysis is evaluated.

It has been found that the stability of a compressible flow increases when the Mach number at the inlet, the loading factor, and the frequency are increased. The active power density is reduced up to 20 per cent in the range

of conditions appropriated for power generations at 60 cps and a loading factor equal to 0.50. Then, with stability assured, the problem of understanding the a.c. energy conversion properties can be treated in the case of a steady-state incompressible fluid model.

SECTION I

INTRODUCTION

I.1 Brief History

Large scale commercial and space power generation systems must, in general, produce a.c. power in order to eliminate excessive transmission losses and to permit efficient transformation to various output voltage levels. Of all the MHD energy conversion devices currently proposed, the d.c. Faraday type generator has been advanced to a position of technological pre-eminence without consideration of the expensive and inefficient inversion equipment necessary to produce the required a.c. power¹. Thus, application of d.c. generators to efficient and inexpensive conversion systems is questionable, except in special cases where d.c. power is required.

It is therefore natural to turn our attention to magnetohydrodynamic methods for direct generation of a.c. power.

Many a.c. MHD devices have already been proposed²⁻³⁻⁴⁻⁵. As in the conventional machine analysis, the problem has been treated as a steady-state problem, with incompressible fluid. However, in any magnetohydrodynamic generator which uses an ionized gas, the effect of compressibility must be included, if there is a large pressure drop through the generator.

The study of the influence of compressibility in direct-current MHD machines has been undertaken by many authors; for example, G. Sutton, who used the assumptions of quasi-one-dimensional flow and small magnetic Reynolds number. However, no study of compressible flow in a.c. MHD generators has been reported, and the detailed effects of compressibility are largely unknown.

I.2 The Object and Scope of This Thesis

The object of this thesis is to present an approach to the evaluation of the perturbations which occur in an a.c. compressible fluid model, i.e., the stability of the system. In Section II, general MHD equations for an a.c.

compressible fluid model are stated in the approximation of the quasi-one-dimensional analysis.

Section III is the development of the MHD equations stated in the approximation of the quasi-one-dimensional analysis. These equations, as well as the unknowns, may be split into time-average parts and time-varying parts.

The time-average parts play the same role as do the d.c. parts in the d.c. compressible fluid model. Assuming a constant average velocity and loading factor, we will design the shape of the channel of a d.c. self-excited MHD generator, from these equations. We will operate this self-excited generator with an alternating current source with the current amplitude adjusted so that the time-average quantities (pressure, velocity, etc....) are the same as for the d.c. generator above.

We will consider time-varying terms in equations of motion as perturbations on the time-average quantities. In Section IV we will evaluate the perturbation quantities; the time-varying equations will be linearised by neglecting all products of the small perturbation amplitudes. The validity of this approximation will be evaluated in Section V.

In Section VI, we will evaluate the effects of perturbations on the output electrical power.

SECTION II

MHD EQUATIONS IN A QUASI ONE-DIMENSIONAL ANALYSIS

II.1 The Equations of Conservation

The MHD equations in a three-dimensional analysis are well known. In this work, we will use MHD equations in a one-dimensional analysis taking into account the variation of the channel cross-section. There is only one space variable. The equations of conservation are first stated by writing the conservation of the properties of the fluid in an elementary volume element, $A dx$. The details of the calculation are presented in Appendix.

For total derivative, we will use the notation: D/dt . The inlet quantities are designated by the subscript i .

The conservation of mass gives:

$$\frac{d(\rho u A)}{dx} = - A \frac{\partial \rho}{\partial t} \quad (1)$$

or

$$\frac{D\rho}{dt} = - \rho \left(\frac{D}{dt} \ln A + \frac{\partial u}{\partial x} \right) \quad (2)$$

where A is the area of the channel, u the velocity and ρ the density.

The conservation of momentum gives:

$$\rho \frac{Du}{dt} = - BJ - \frac{\partial P}{\partial x} \quad (3)$$

where B is the magnetic flux density, J the current density, P the mechanical pressure.

The conservation of energy gives:

$$\rho \frac{D}{dt} \left(h + \frac{u^2}{2} \right) - \frac{\partial P}{\partial t} = - EJ \quad (4)$$

This expression will be written in terms of entropy from equations (3) and (4)

$$R\left(\frac{\gamma}{\gamma-1}\right) \frac{DT}{dt} - \frac{RT}{P} \frac{DP}{dt} = \frac{1}{\rho} \frac{J^2}{\sigma} = T \frac{DS}{dt} \quad (5)$$

where T is the temperature, σ the conductivity, R the specific gas constant, γ the ratio of specific heats.

II.2 The General MHD Equation

The three complementary equations we need are "local equations" for which the variation of the channel area is not taken into account. These are:

Ohm's law:

$$J = \sigma (uB - E) \quad (6)$$

the approximate expression of the conductivity:

$$\sigma = \sigma_1 \left(\frac{T}{T_1}\right)^\epsilon \left(\frac{P_1}{P}\right)^{1/2} \quad (7)$$

if we neglect electron-ion collision, and where:

$$\epsilon = \frac{3}{4} + \frac{E_i}{2KT_1} \left(1 - \frac{T_1}{T}\right) \text{Ln}^{-1}\left(\frac{T}{T_1}\right) \quad (8)$$

E_i being the ionization energy, and K Boltzmann's constant.

The gas law: If the degree of ionization is assumed small, one may reasonably assume that the gas is perfect and follows the equation:

$$P = \rho R T \quad (9)$$

SECTION III

TIME AVERAGE EQUATIONS - DESIGN OF A COMPRESSIBLE FLUID CHANNEL WITH CONSTANT VELOCITY AND CONSTANT LOADING FACTOR

The MHD equations, determined in Section II, will be split into time-average parts (subscript o) and time-varying parts (subscript 1), as will the unknowns. For instance, $u \rightarrow u_o(x) + u_1(x,t)$. The time-average parts play the same role as does the d.c. part in a d.c. compressible fluid model. Then we can design the shape of the channel of a d.c. self-excited MHD generator, with constant velocity and constant loading factor, and consider that the time-varying part of the MHD equations represents the perturbations on the time-average quantities.

III.1 Shape of the Channel of a d.c. Self-Excited Generator

The problem of defining the dimensions of the channel is illustrated in Figure 1. The basic assumptions are the following:

- 1) To simplify the problem, one neglects the effects of friction and heat transfer.
- 2) One assumes that the magnetic Reynolds number based on length is small compared to unity.
- 3) The magnetic circuits are closed by highly permeable, non-conducting magnetic material.

To solve the problem, we must determine the nine unknowns:

geometrical:	w, d
electrical:	J_o, B_o, E_o, σ_o
thermodynamical:	P_o, ρ_o, T_o

We already know six equations from Section I:

$$\text{conservation of mass: } \rho_o(wd) = \rho_{o1}(wd)_1 \quad (10)$$

$$\text{conservation of momentum: } \frac{dP_o}{dx} = - B_o J_o \quad (11)$$

$$\text{conservation of energy: } \rho_o u_o c_p \frac{dT_o}{dx} = - E_o J_o \quad (12)$$

$$\text{Ohm's law: } J_o = v_o(u_o B_o - E_o) \quad (13)$$

$$\text{conductivity: } \sigma_o = \sigma_{o1} \left(\frac{T_o}{T_{o1}} \right)^\epsilon \left(\frac{P_{o1}}{P_o} \right)^{1/2} \quad (14)$$

$$\text{equation of state: } P_o = \rho_o R T_o \quad (15)$$

and we get three equations, relative to the assumptions above:

$$\text{flux density: } B_o d = (B_o d) \quad (16)$$

$$\text{constant loading factor } k: E_o = k u_o B_o \quad (17)$$

$$\text{constant voltage: } E_o W = (E_o W)_1 \quad (18)$$

Assuming a small magnetic Reynolds number compared to unity, we neglect the magnetic field generated by current flow in the gas. The results take the form:

$$\frac{P_o}{P_{o1}} = \left(\frac{\rho_o}{\rho_{o1}}\right)^{\frac{1}{1-\alpha}} = \left(\frac{A}{A_1}\right)^{-\frac{1}{1-\alpha}} = \left(\frac{T_o}{T_{o1}}\right)^{\frac{1}{\alpha}} = \left(\frac{m_o^2}{m_{o1}^2}\right)^{-\frac{1}{\alpha}} = \left(\frac{d}{d_1}\right)^{-\frac{2}{1-\alpha}} = \left(\frac{w}{w_1}\right)^{-\frac{2}{1-\alpha}} \quad (19)$$

with

$$\alpha = k \frac{\gamma-1}{\gamma} \quad (20)$$

m_o being the Mach number.

The ratio P_o/P_{o1} takes the form:

$$\frac{P_o}{P_{o1}} = \left(1 + \frac{\lambda}{L} x\right)^{-\frac{1}{\lambda}} \quad \dots \text{ if } \lambda \neq 0 \quad (21)$$

$$\frac{P_o}{P_{o1}} = e^{-\frac{x}{L}} \quad \dots \text{ if } \lambda = 0 \quad (22)$$

where

$$\lambda = -\frac{1}{2} + (\epsilon-1) k \frac{\gamma-1}{\gamma} \quad (23)$$

$$L = \frac{P_{o1}}{(1-k) (\sigma_o B_o^2)_1 u_o} \quad (24)$$

L is generally called "interaction length" ⁶. Figures 2 and 3 give the variations of P_o/P_{o1} and of λ for different values of k and ϵ .

SECTION IVa

PERTURBATION EQUATIONS - SMALL AMPLITUDE ANALYSIS

We operate the self-excited d.c. generator with an a.c. current source of frequency ω , for which the current amplitude is adjusted so that the root-mean-square quantities (pressure, velocity...) are the same as for the d.c. self-excited generator in Section III above.

The magnetic Reynolds number is small compared to 1 so that the induced magnetic field may be neglected.

In these assumptions, the electrical quantities may be split as:

$$B(x,t) = \text{Re} \left\{ B_0(x) \sqrt{2} \exp(j\omega t) \right\} \quad (25)$$

$$E(x,t) = \text{Re} \left\{ E_0(x) \sqrt{2} \exp(j\omega t) + E_1(x,t) \right\} \quad (26)$$

$$J(x,t) = \text{Re} \left\{ J_0(x) \sqrt{2} \exp(j\omega t) \right\} \quad (27)$$

$$\sigma(x,t) = \sigma_0(x) + \sigma_1(x,t) \quad (28)$$

The MHD equations in a quasi-one-dimensional analysis may be split into time-average equations (Section III) and time-varying equations which play the role of perturbation equations on the time-average equations.

We have six unknowns: P_1 , u_1 , ρ_1 , T_1 , E_1 , σ_1 , for six linearised perturbation equations which are:

$$\text{conservation of mass:} \quad \frac{D_0}{dt} \left(\frac{\rho_1}{\rho_0} \right) + u_0 \frac{\partial}{\partial x} \left(\frac{u_1}{u_0} \right) = 0 \quad (29)$$

$$\text{conservation of momentum:} \quad \rho_0 \frac{D_0}{dt} (u_1) = -(B_0 J_0) \exp(2j\omega t) - \frac{\partial P_1}{\partial x} \quad (30)$$

conservation of energy:
$$\frac{(J_0)^2}{\sigma_0} \exp(2j\omega t) = - \left(\frac{D_0}{dt} (P_1) + u_1 \frac{\partial P_0}{\partial x} \right) + c_p \left(\rho_0 \left(\frac{D_0}{dt} T_1 + u_1 \frac{\partial T_0}{\partial x} \right) + \rho_1 \left(\frac{D_0}{dt} T_0 \right) \right) + c_p \frac{\sigma_1}{\sigma_0} \rho_0 \frac{D_0}{dt} T_0 - \frac{\sigma_1}{\sigma_0} \frac{D_0}{dt} P_0 \quad (31)$$

where D_0/dt is the unperturbed operator $\left(\frac{\partial}{\partial t} + u_0 \frac{\partial}{\partial x} \right)$.

linearised conductivity gas law:
$$\frac{\sigma_1}{\sigma_0} = \epsilon \frac{T_1}{T_0} - \frac{1}{2} \frac{P_1}{P_0} \quad (32)$$

linearised Ohm's law:
$$- \frac{\sigma_1}{\sigma_0} u_0 B_0 \sqrt{2(1-k)} \exp(j\omega t) = \frac{u_1}{u_0} u_0 B_0 \sqrt{2} \exp(j\omega t) - E_1 \quad (33)$$

linearised gas law:
$$\frac{P_1}{P_0} = \frac{\rho_1}{\rho_0} + \frac{T_1}{T_0} \quad (34)$$

These equations show that the electrical perturbations oscillate at an odd frequency and the thermodynamical perturbations at an even frequency.

An easy way to solve the perturbation equations is to introduce normalized variables, and to eliminate time dependence, by assuming an appropriate frequency for the variables as suggested by the remark above.

$$P_1(x, t) = \text{Re}\{P_1(x) \exp(2j\omega t)\} \quad (35)$$

$$\rho_1(x, t) = \text{Re}\{\rho_1(x) \exp(2j\omega t)\} \quad (36)$$

let us assume:
$$T_1(x, t) = \text{Re}\{T_1(x) \exp(2j\omega t)\} \quad (37)$$

$$u_1(x, t) = \text{Re}\{u_1(x) \exp(2j\omega t)\} \quad (38)$$

$$\sigma_1(x, t) = \text{Re}\{\sigma_1(x) \exp(2j\omega t)\} \quad (39)$$

and introduce:

$$\bar{P} = P_1/P_0$$

$$\bar{\rho} = \rho_1/\rho_0$$

$$\bar{T} = T_1/T_0$$

$$\bar{u} = u_1/u_0$$

$$\bar{\sigma} = \sigma_1/\sigma_0$$

then:

$$P_1 = \text{Re} \left(\bar{P} P_0 \exp (2j\omega t) \right) \quad (40)$$

$$\rho_1 = \text{Re} \left(\bar{\rho} \rho_0 \exp (2j\omega t) \right) \quad (41)$$

$$T_1 = \text{Re} \left(\bar{T} T_0 \exp (2j\omega t) \right) \quad (42)$$

$$u_1 = \text{Re} \left(\bar{u} u_0 \exp (2j\omega t) \right) \quad (43)$$

$$\sigma_1 = \text{Re} \left(\bar{\sigma} \sigma_0 \exp (2j\omega t) \right) \quad (44)$$

Finally we obtain the following equations:

a. Ohm's law:

(45)

$$\bar{u} u_0 B_0 \sqrt{2} \exp (j\omega t) - E_1 = -\bar{\sigma} u_0 B_0 \sqrt{2}(1-k) \exp (j\omega t)$$

b. conductivity:

$$\bar{\sigma} = \epsilon \bar{T} - \frac{\bar{P}}{2}$$

c. conservation of mass:

$$(2j\omega\bar{\rho} + u_o \frac{d\bar{\rho}}{dx}) + u_o \frac{d\bar{u}}{dx} = 0$$

d. conservation of momentum:

$$u_o \rho_o (2j\omega\bar{u} + u_o \frac{d\bar{u}}{dx}) + P_o \frac{d\bar{P}}{dx} + (1-\bar{P})(B_o J_o) = 0$$

e. conservation of energy:

$$P_o (2j\omega (\frac{\gamma}{\gamma-1} \bar{T} - \bar{P}) + u_o \frac{d}{dx} (\frac{\gamma}{\gamma-1} \bar{T} - \bar{P})) + B_o J_o u_o (1-k) (\bar{u} + \frac{\bar{P}}{2} + \epsilon \bar{T} - 1) = 0$$

f. gas law:

$$\bar{P} = \bar{\rho} + \bar{T}$$

In a first approximation, we assume that the relative perturbation of the conductivity $\bar{\sigma}$ is negligible with respect to 1. The simplified equations become then:

Ohm's law:

$$E_1 = \bar{u} u_o B_o \sqrt{2} \exp(j\omega t) \quad (46)$$

mass conservation:

$$2j\omega\bar{\rho} + u_o \frac{d\bar{\rho}}{dx} = - u_o \frac{d\bar{u}}{dx} \quad (47)$$

momentum conservation:

$$\rho_o u_o (2j\omega\bar{u} + u_o \frac{d\bar{u}}{dx}) = - P_o \frac{d\bar{P}}{dx} + B_o J_o (\bar{P}-1) \quad (48)$$

energy conservation:

$$\frac{c_p}{R} (2j\omega\bar{T} + u_o \frac{d\bar{T}}{dx}) - (2j\omega\bar{P} + u_o \frac{d\bar{P}}{dx}) + \frac{u_o B_o J_o}{P_o} (1-k) (\bar{P} + \bar{u} - 1) = 0 \quad (49)$$

gas law:

$$\bar{P} = \bar{\rho} + \bar{T} \quad (50)$$

where all functions with the subscript o are given by Part III and where the five unknowns: E_1 , \bar{u} , \bar{P} , $\bar{\rho}$, \bar{T} have to be determined.

SECTION IVb

INTEGRATION OF THE VELOCITY PERTURBATION
EQUATION IN SOME PARTICULAR CASES

IVb.1 The Velocity Perturbation Equation

We have set up a system of five perturbation equations for five perturbed quantities:

$$\bar{u} \quad \bar{\rho} \quad \bar{P} \quad \bar{T} \quad E_1$$

which can be solved step by step by elimination of the variables. For instance, the elimination of $\bar{\rho}$, \bar{T} and E_1 leads to a linear system of differential equations of first order. Following Woodson⁴, these can be written, in matrix form, as:

$$\frac{d}{dx} \{\bar{u}, \bar{P}\} = \bar{S}(x) \{\bar{u}, \bar{P}\} + \bar{T}(x) \quad (51)$$

with the following expression for the matrix

$$\bar{S} = \left[\begin{array}{cc} \frac{(-\frac{K}{L} y^\lambda + \gamma m_1^2 \bar{a} y^{-\alpha})}{\gamma(1 - m_1^2 y^{-\alpha})} & -\frac{(\frac{1+K}{L} y^\lambda + \bar{a})}{\gamma(1 - m_1^2 y^{-\alpha})} \\ \frac{-\frac{K}{L} y^\lambda + \gamma \bar{a}}{1 - \frac{y^\alpha}{m_1^2}} & -\frac{\frac{1}{L} (K + \frac{y^\alpha}{m_1^2}) y^\lambda + \bar{a}}{1 - \frac{y^\alpha}{m_1^2}} \end{array} \right] \quad (52)$$

and

$$\bar{T} = \left\{ \left(\frac{d\bar{u}}{dx} \right)_1, \left(\frac{d\bar{P}}{dx} \right)_1 \right\} = \left\{ -\frac{1 - \alpha}{(m_1^2 - 1) L}, \frac{1 + Km_1^2}{(m_1^2 - 1) L} \right\} \quad (53)$$

and where:

$$y = \frac{P_0}{P_{01}} \text{ is the function } \left\{ \begin{array}{ll} \left(1 + \frac{\lambda}{L} x \right)^{-\frac{1}{\lambda}} & \text{for } \lambda \neq 0 \\ \exp - \frac{x}{L} & \text{for } \lambda = 0 \end{array} \right.$$

m_1 is the Mach number at the inlet

$$K \text{ is a constant} = (1-k)(\gamma-1) \quad (54)$$

$$\bar{a} \text{ is a complex constant} = 2j\omega/u_0 \quad (55)$$

$$\alpha \text{ is a constant} = k(\gamma-1)/\gamma \quad (56)$$

The solution of equation (51) takes the form:

$$\{\bar{u}, \bar{P}\} = \Omega(\bar{S}) Q_0^x \{ \Omega^{-1}(\bar{S}) \bar{T} \} \quad (57)$$

where $\Omega(\bar{S})$ is the matrizant of \bar{S} . Practically, the evaluation of $\Omega(\bar{S})$ is rather difficult owing to an indefinite integration, giving a series expansion of $\Omega(\bar{S})$, but it appears under this form that

$$\{ |\bar{u}|, |\bar{P}| \} < \left\{ \left| \left(\frac{d\bar{u}}{dx} \right)_1 \right|, \left| \left(\frac{d\bar{P}}{dx} \right)_1 \right| \right\} x \quad (58)$$

This and the graphs of Figure 4 representing the variation of the modulus of the derivatives $|(d\bar{u}/dx)_1|$ and $|(d\bar{P}/dx)_1|$ show that a more severe limitation occurs for the pressure perturbation than for the velocity perturbation. In fact, the velocity perturbation may cause physical effects like shock waves. These velocity perturbations will be determined later, instead of the pressure perturbation.

From equation (51) we get the velocity perturbation equation:

$$A \frac{d^2 \bar{u}}{dx^2} + \left(\frac{dA}{dx} - \frac{A}{Q} \frac{dQ}{dx} + C + \frac{AF}{D} \right) \frac{d\bar{u}}{dx} + \left(\frac{dC}{dx} - \frac{C}{Q} \frac{dQ}{dx} + \frac{CF - QG}{D} \right) \bar{u} =$$

$$\left(\frac{dN}{dx} - \frac{N}{Q} \frac{dQ}{dx} + \frac{NF - QH}{D} \right) \bar{u} \quad (59)$$

with

$$A = (1 - m_1^2 y^{-\alpha}) \gamma \quad D = (1 - \frac{y^\alpha}{m_1^2})$$

$$Q = (\frac{1+K}{L} y^\lambda + \bar{a}) \quad F = \bar{a} + (K + \frac{y^\alpha}{m_1^2}) \frac{y^\lambda}{L}$$

$$C = (\frac{K}{L} y^\lambda - \bar{a} \gamma m_1^2 y^{-\alpha}) \quad G = (\frac{K}{L} y^\lambda - \gamma \bar{a})$$

$$N = (\frac{1+K}{L} y^\lambda) \quad H = (K + \frac{y^\alpha}{m_1^2}) \frac{y^\lambda}{L}$$

(60)

m_1 being the Mach number at the inlet.

From equation (60) with five independent parameters, we can determine the coefficients of the equation. Let us take for instance:

k , σ_{01} , P_{01} , u_0 and f the frequency.

The knowledge of:

k gives α and K from (54) and (56).

σ_{01}

gives ϵ , λ and T_{01} for a given gas

P_{01}

u_0 gives m_1^2 , L

f gives \bar{a}

If we take three of five parameters, say σ_{01} , P_{01} and (u_0) then equation (59) will depend on two parameters: loading factor (k) and frequency (f), and the integration will be done for different values of these two basic parameters. But before we calculate a numerical solution of (59), we shall study a case of special interest, namely that of an open circuit.

For $k = 1$ the velocity equation gives

$$\gamma(1 - m_1^2) \frac{d^2 \bar{u}}{dx^2} - (2\gamma m_1^2 \bar{a}) \frac{d\bar{u}}{dx} - (\gamma m_1^2 \bar{a}^2) \bar{u} = 0$$

for which we get the trivial solution,

$$\bar{u} = 0 \tag{61}$$

Then, from (46), (47), (48), (49), (50):

$$\bar{P} = 0 = \bar{\rho} = \bar{T} = E_1$$

Consequently, there is no perturbation in an open circuit generator.

Later we integrate (59) numerically for values of $k \neq 1$, and for some particular cases where the integration becomes easy and can be done by hand.

The numerical application in each of the particular cases below will be done for a combustion gas having the properties:

$$\sigma_{01} = 21.9 \text{ mho/m at pressure } P_{01}$$

$$u_{01} = 1430 \text{ m/sec}$$

$$P_{01} = 5 \times 10^5 \text{ Newton/m}^2$$

and where:

$$\epsilon = 12$$

$$T_{01} = 3000 \text{ }^\circ\text{K}$$

$$B_{01} = 4 \text{ wb/m}^2$$

$$m_1^2 = 1.5$$

We use a supersonic velocity so that the downward perturbations cannot go up. Therefore, at the inlet boundary, there are no perturbations. But the derivatives of the perturbations are not zero. Their magnitude is given by Figure 4.

IVb.1.1 Large Frequency

For large frequency ($f \geq 500$ cps) and for $x < 4\text{m}$, the velocity equation takes a simple form:

$$\left(1 - \frac{1}{m_1^2}\right) \frac{d^2 \bar{u}}{dx^2} + (2\bar{a}) \frac{d\bar{u}}{dx} + (\bar{a}^2) \bar{u} = - \left(\frac{\bar{a}}{\gamma m_1^2 L}\right)$$

for which the solution is:

$$\bar{u} = -\frac{1}{\gamma a m_1^2 L} + c_1 \exp\left(-\frac{m_1}{m_1 + 1} \bar{a}x\right) + c_2 \exp\left(-\frac{m_1}{m_1 - 1} \bar{a}x\right) \quad (62)$$

c_1 and c_2 being constants.

The solution is composed of two waves oscillating at frequency:

$$\frac{2\omega}{u_0} \left(\frac{m_1}{m_1 + 1}\right) \quad \text{and} \quad \frac{2\omega}{u_0} \left(\frac{m_1}{m_1 - 1}\right)$$

Figure 5 shows the representations of \bar{u}_r and \bar{u}_c for $k = 1/2$ and for $f = 960$ cps. We deduce from expression (62) that when the frequency increases, then the perturbations decrease, so that it becomes more interesting to operate at large frequency than at small frequency.

IVb.1.2 Zero-Order Approximation

Equation (59) can be easily integrated when the coefficients are constants, and in fact, we can always expand the coefficients of (59) close to the origin and then determine the degree of approximation we allowed ourselves in assuming constant coefficients (zero-order approximation). To this purpose, we take the ratio between the first two terms in the development, close to the origin, of each of the coefficients of equation (59). Then, we plot the minimum value of the modulus of these ratios for different values of k and f . The minimum value of the modulus occurs for the coefficient of \bar{u} but not for the other three coefficients. This minimum has a value of 0.92 at a frequency of 114 cps, in the case of a short circuit. This is quite a severe limitation to the zero-order validity.

Once the validity of the zero-order solution is known, then we can integrate equation (59). The solution will take the form:

$$\bar{u} = \bar{u}_p + c_1 \exp(r_1 x) + c_2 \exp(r_2 x) \quad (63)$$

where \bar{u}_p designates the complex particular solution, and c_1, c_2 and r_1, r_2 are complex constants determined by (59). The numerical application has been done for

$$k = 0 \quad 0.5 \quad 0.8$$

$$f = 0 \quad 28.5 \quad 57 \quad 114 \text{ cps}$$

The results are given under the form of \bar{u}_r, \bar{u}_c vs. x where \bar{u}_r is the real part of \bar{u} and \bar{u}_c is the imaginary part of \bar{u} (Figures 7, 8, 9, 10).

IVb.1.3 General Case

The integration above is valid for a range of x less than $2m$. For $x > 2m$, the velocity equation can be integrated by a power series expansion of the form:

$$\bar{u} = \sum_{k=0}^{\infty} \alpha_k x^k$$

where α_k is a complex number.

But it appears that a large number of terms are then necessary, so that hand calculation becomes impractical. A detailed study of equation (57) would allow a closer approach of the solution.

However, the determination of the solution of the velocity perturbation equation is limited by the fact that we operate in a linear small-amplitude analysis. The next step of our work is to determine the degree of validity of the small-amplitude analysis for the values of our parameters k and f .

SECTION V

VALIDITY OF THE SMALL-AMPLITUDE ANALYSIS IN THE ZERO-ORDER APPROXIMATION

We have seen that the perturbation of the velocity in a.c. operation of a self-excited generator is given by

$$u_1 = \text{Re}(\bar{u}u_0 \exp(2j\omega t))$$

where \bar{u} has been determined in Part IV. The small-amplitude analysis holds for the assumption of $|\bar{u}| \ll 1$.

In this chapter, from the numerical value of \bar{u} obtained in Section IV, we determine the variation of $|\bar{u}|$ along the channel, for a range of x less than 2 metres.

At the origin we note that:

$$\left(\frac{d|\bar{u}|}{dx}\right)_1 = \left|\left(\frac{d\bar{u}}{dx}\right)_1\right|$$

The values of $\left|\frac{d\bar{u}}{dx}\right|_1$ are tabulated on the graph 4.

Graphs 7, 8b, 9b and 10b represent the variation of $|\bar{u}|$ along the channel in the zero-order approximation for

$$k = 0 \quad 0.5 \quad 0.8 \quad 1$$

$$f = 0 \quad 28.5 \quad 57 \quad 114 \text{ cps}$$

In Figure 11 we have plotted the maximum value of $|\bar{u}|$ for the range of x less than 2 metres, which gives us the validity of linear analysis of small perturbations.

We note that if we do not want a velocity less than the sound velocity (a_s) then:

$$a_s < u_o - |u_1|$$

Hence,

$$(1 - |\bar{u}|) > \frac{a_s}{u_o}$$

This implies that:

$$|\bar{u}| < 1 - \frac{1}{m}$$

But it appears that the required condition, $|\bar{u}|_{\max} < 1 - \frac{1}{m_1}$, is sufficient.

Figure 11 shows the limitation of $|\bar{u}|_{\max}$ vs. $1 - \frac{1}{m_1}$. The graph shows that, for a Mach number at the entrance equal to 1.225, and for an industrial frequency of 60 cps, the loading factor must be at least equal to 0.8. For a loading factor equal to 0.5, the operating frequency must be at least 110 cps. Hence, it would be interesting to use large values of velocity and frequency, so as to avoid limitations perturbations.

SECTION VI

THE PROBLEM OF THE ELECTRICAL OUTPUT POWER

In this chapter we evaluate the influence of the compressibility on the active and reactive power.

We already stated that:

$$E = E_0 \sqrt{2} \cos \omega t + E_1 \quad (64)$$

with

$$E_1 = \operatorname{Re}(u_1 B_0 \sqrt{2} \exp j\omega t) \quad (65)$$

$$u_1 = \operatorname{Re}((\bar{u}_r + j\bar{u}_c) u_0 \exp 2j\omega t) \quad (66)$$

Then,

$$\begin{aligned} E = E_0 + \frac{\sqrt{2}}{2} u_0 B_0 (\bar{u}_r \cos \omega t - \bar{u}_c \sin \omega t) \\ + \frac{\sqrt{2}}{2} u_0 B_0 (\bar{u}_r \cos 3\omega t - \bar{u}_c \sin 3\omega t) \end{aligned}$$

and can be written as:

$$E = \operatorname{Re}(E_\omega \exp j\omega t + E_{3\omega} \exp 3j\omega t) \quad (67)$$

with:

$$E_{\omega} = E_0 \sqrt{2} \left(1 + \frac{u_R}{2k} \right) - j \frac{u_C}{2k} \quad (68)$$

$$E_{3\omega} = E_0 \sqrt{2} \left(\frac{\bar{u}_R}{2k} - j \frac{\bar{u}_C}{2k} \right) \quad (69)$$

J, in a similar manner, takes the form:

$$J = \text{Re}(J_0 \sqrt{2} \exp j\omega t) \quad (70)$$

The complex form of Poynting's theorem⁷, gives an expression for the active and reactive power density. For a frequency (2ω), we get:

$$\begin{aligned} - \text{Re}(\text{div } \vec{S}) &= \frac{1}{2} \text{Re}(E_{\omega} J_0 \sqrt{2}) \\ &= E_0 J_0 \left(1 + \frac{u_R}{2k} \right) \end{aligned} \quad (71)$$

and,

$$\begin{aligned} - \text{Im}(\text{div } \vec{S}) &= \frac{1}{2} \text{Im}(E_{\omega} J_0 \sqrt{2}) + \omega \frac{B_0^2}{\mu_0} \\ &= - E_0 J_0 \left(\frac{\bar{u}_C}{k} \right) + \omega \frac{B_0^2}{\mu_0} \end{aligned} \quad (72)$$

where \vec{S} is the Poynting vector.

The right-hand side of equation (71) represents the average density of active power.

The first term on the right-hand side of equation (72) is the reactive power density associated with the average power density of equation (71). The second term represents the average reactive power stored within the field in the channel.

For a range of frequency less than 100 cps and a length less than 2 metres, \bar{u}_r appears to be negative and \bar{u}_c positive.

From (71), we deduced that the generated average density of active power is reduced from the unperturbed case. But from (72) it appears that the need of reactive power density is less than in the case of steady-state with no perturbation.

Figures 12 and 13 show the maximum decrease of relative active and reactive power density due to the gas compressibility. The change of generated active power is of the order of 20 per cent, while the change in reactive power requirement does not exceed 2 per cent in the range of conditions appropriated for power generation at 60 cps and a loading factor equal to 0.5.

However, for large values of the frequency, \bar{u}_p may take positive values (see Figure 5). This may enhance the production of the active power density, as it can be explained by an increase in the stability of the flow.

SECTION VII

CONCLUDING REMARKS

The results of the analysis of the perturbations which occur in a self-excited a.c. MHD generator, in the small-amplitude approximation, are still valid for a.c. conduction-type generators, for which an analysis has been made in the case of steady incompressible flow with sinusoidal variation of electrical quantities. However, the reactive power required for a self-excited a.c. MHD generator makes it desirable to design new MHD machines for generating a.c. power without external reactive power requirements.

Such a new concept of MHD conduction machines for a.c. power generation has been proposed and analysed by Woodson⁵. It was shown that two conduction-type generators can be cross-coupled in such a way that the reactive field winding of one machine provides a capacitive tuning for the other machine. The basic system proposed by Woodson consists of a channel of constant cross-section. The velocity and conductivity of the conducting fluid are assumed constant. The channel contains two pairs of electrodes forming two conduction generators. The addition of two cross-coupling windings transforms the pair of self-excited d.c. generators into a two-phase self-excited a.c. generator, and under certain conditions of operation there are steady-state alternating currents. In each of these two devices the magnetic field leads the electric field by $\pi/4$ radians. But the magnitude of the modulus of the velocity perturbations is still the same and the analysis of the curves of Figure 11 remains valid.

It has been shown that the stability of the compressible flow increases when the Mach number at the inlet, the loading factor, and the frequency are increased. The Mach number at the entrance must be greater than a certain lower limit (Figure 11) in order that the downstream velocity does not become subsonic. For example, for a frequency of 60 cps and a loading factor equal

to $1/2$, the inlet Mach number must be greater than 1.6. The compressibility greatly affects the output electric power density as shown on Figures 12 and 13, where we have represented the maximum per cent of decrease in active and reactive power for a range of 2 metres length, as deduced from the equations (71) and (72). These figures show the benefit of increasing the loading factor and the frequency to reduce the relative decrease of electrical output power caused by the gas compressibility. Assuming a certain degree of stability defined by Figure 11, it would be possible to treat the problem of a.c. energy conversion properties for conditions of incompressible flow and steady-state operation.

More work remains to be done in evaluating the value of the velocity perturbation along the channel in the small-amplitude approximation with the use of numerical computation. To what extent this analysis remains true and how to treat the case of large perturbations is still open for further theoretical work.

APPENDIX

MHD EQUATIONS OF CONSERVATION IN A QUASI ONE-DIMENSIONAL ANALYSIS

The conservation of mass is stated for an elementary volume element ($A \Delta x$), inside which we average the variables.

$$\Delta(\rho u A) + A \Delta x \frac{\partial \rho}{\partial t} = 0 \quad (\text{A.1})$$

or:
$$\frac{d(\rho u A)}{dx} + A \frac{\partial \rho}{\partial t} = 0 \quad \text{at the limit} \quad (\text{A.2})$$

The conservation of momentum is stated in the same way, for a volume element:

$$\Delta((P + \rho u^2) A) - P \Delta A + A \Delta x \left(\frac{\partial}{\partial t} \rho u \right) = 0 \quad (\text{A.3})$$

or, with the help of (A.2):

$$\rho \frac{D}{dt} u = - B J - \frac{\partial P}{\partial x} \quad (\text{A.4})$$

The conservation of energy gives

$$\Delta\left(\rho u A \left(h + \frac{u^2}{2}\right)\right) + A \Delta x \left(\frac{\partial}{\partial t} \rho \left(U + \frac{u^2}{2}\right) + E J\right) = 0 \quad (\text{A.5})$$

where U designates the internal energy of the gas, and with the help of (A.2):

$$\rho \frac{D}{dt} \left(h + \frac{u^2}{2}\right) - \frac{\partial P}{\partial x} = - E J \quad (\text{A.6})$$

REFERENCES

1. Sporn, P.
Kantrowitz, A.R. Large-Scale Generation of Electric Power by Application of the Magnetohydrodynamic Concept, *Power*, November, 1959.
2. Woodson, H.H.
Wilson, G.L.
Lewis, A.T. A Study of Magnetohydrodynamic Parametric Generators, *Proceedings of the Third Symposium on the Engineering Aspects of Magnetohydrodynamics*, Rochester, N.Y., March, 1962.
3. Haus, H.A. Alternating-Current Generation with Moving Conducting Fluids, *Journal of Applied Physics*, June, 1962.
4. Woodson, H.H. Magnetohydrodynamic a.c. Power Generation, *Proceedings of the AIEE Pacific Energy Conversion Conference*, San Francisco, Calif., August, 1962, pp. 30-1 through 30-17.
5. Woodson, H.H. A New Type of Magnetohydrodynamic a.c. Power Generator, Internal Memorandum No. 75, Energy Conversion Group, M.I.T., February 11, 1963.
6. Sutton, G.W. *The Theory of Magnetohydrodynamic Power Generators*, Missile and Space Division, General Electric, Vol. 14, pp. 114-141 (December 1962).
7. Fano, R.M.
Chu, L.J.
Adler, R.B. *Electromagnetic Fields, Energy and Forces*, John Wiley and Sons, New York, 1960, p. 322.

TABLE OF FIGURES

- Figure 1. Perspective of the self-excited MHD generator.
- Figure 2. Relative variation of the pressure through a d.c. MHD channel with constant velocity and loading factor.
- Figure 3. Graph of λ vs. k and ϵ .
- Figure 4. Variation of the magnitude of the derivative of the perturbations at the origin vs. the loading factor.
- Figure 5. Variation of \bar{u}_r and \bar{u}_c for large frequency $f = 960$ cps, $k = 1/2$, $m_1^2 = 3/2$.
- Figure 6. Validity of the zero-order approximation.
- Figure 7. Variation of $|\bar{u}|$ along the channel for a d.c. self-excited MHD generator.
- Figure 8a. Variation of \bar{u}_r, \bar{u}_c along the channel for $f = 28.5$ cps.
- Figure 8b. Variation of $|\bar{u}|$ along the channel for $f = 28.5$ cps.
- Figure 9a. Variation of \bar{u}_r, \bar{u}_c along the channel for $f = 57$ cps.
- Figure 9b. Variation of $|\bar{u}|$ along the channel for $f = 57$ cps.
- Figure 10a. Variation of \bar{u}_r, \bar{u}_c along the channel for $f = 114$ cps.
- Figure 10b. Variation of $|\bar{u}|$ along the channel for $f = 114$ cps.
- Figure 11. Validity of the linear analysis of small perturbation vs. frequency and loading factor.
- Figure 12. Maximum relative decrease of active power due to the gas compressibility.
- Figure 13. Maximum relative decrease of reactive power due to the gas compressibility.

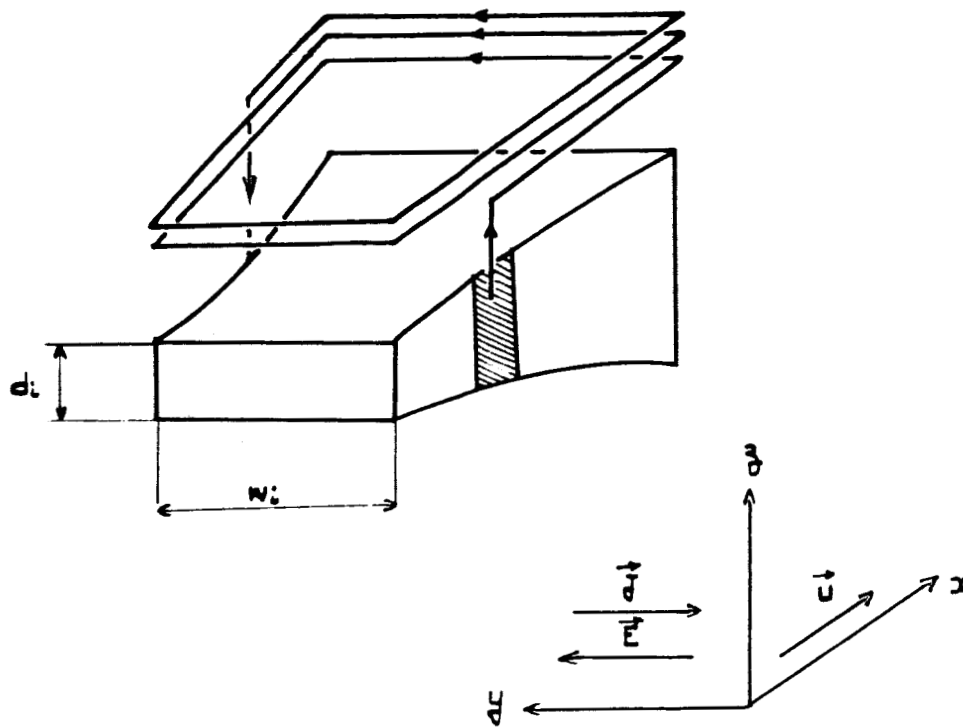


Figure 1.- Perspective of the self-excited MHD generator, showing the channel dimensions.

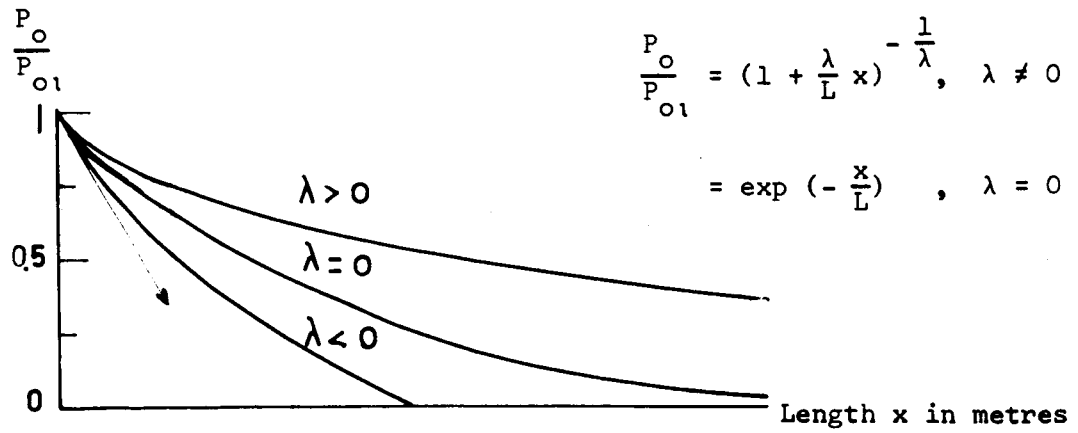
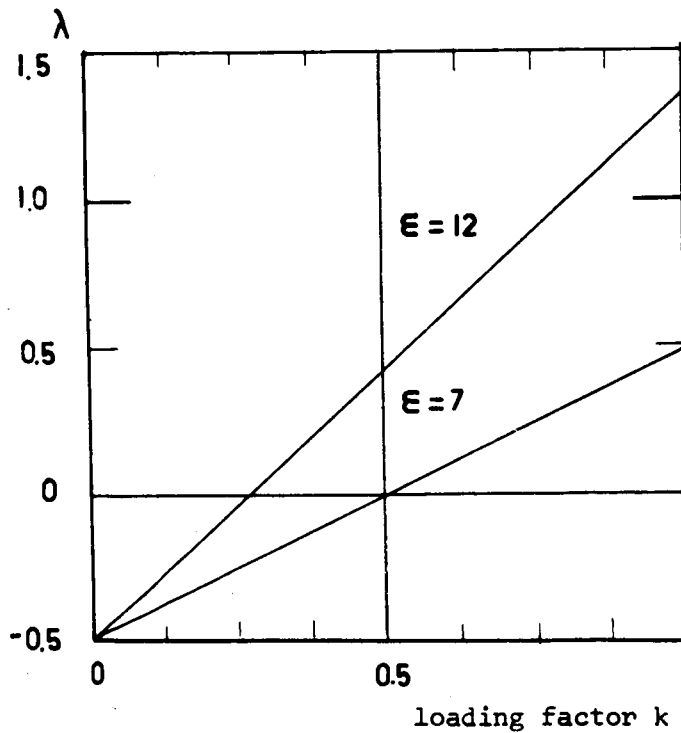
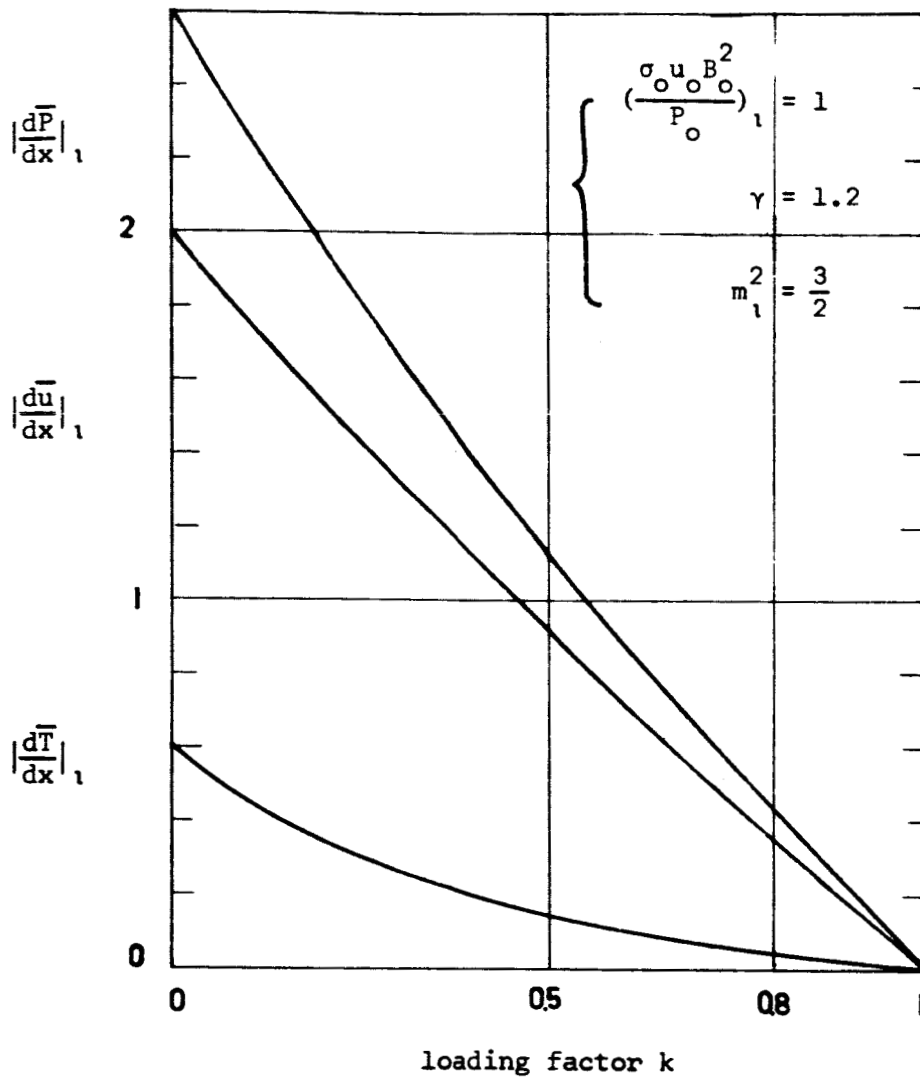


Figure 2.- Relative variation of the pressure through a d.c. MHD channel with constant velocity and constant loading factor.



$$\lambda = -\frac{1}{2} + (\epsilon - 1) k \frac{\gamma - 1}{\gamma}$$

Figure 3.- Variation of λ .



$$\left| \frac{d\bar{P}}{dx} \right|_1 = \frac{1 + (\gamma-1)(1-k) m_1^2}{L(m_1^2-1)}$$

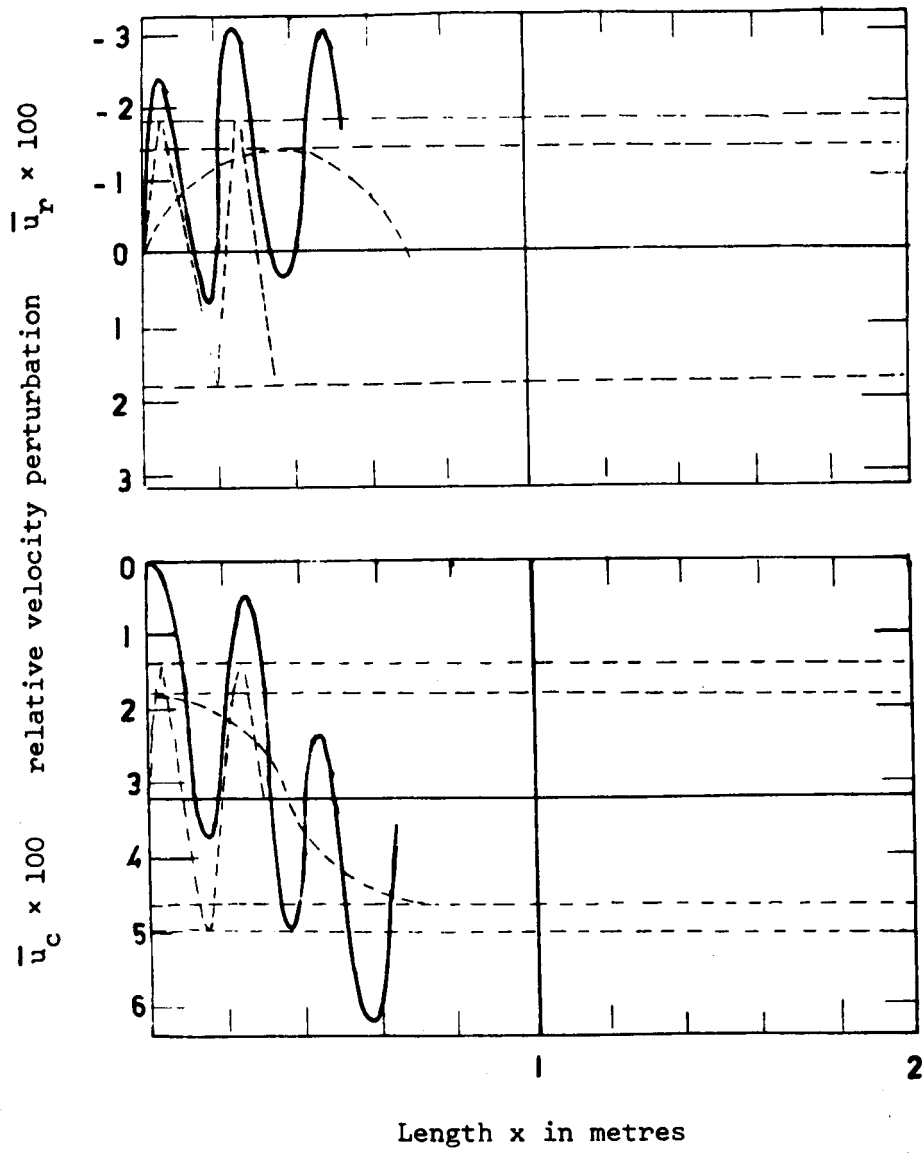
$$\left| \frac{d\bar{u}}{dx} \right|_1 = \frac{1 - k\left(\frac{\gamma-1}{\gamma}\right)}{L(m_1^2-1)}$$

$$\left| \frac{d\bar{T}}{dx} \right|_1 = \frac{m_1^2(\gamma-1)(1-k)}{L(m_1^2-1)}$$

Figure 4.- Magnitude of the derivative of the perturbations at the origin vs. k.

$$\bar{u}_r = -1.4 \times 10^{-2} \sin(4.65x) - 1.76 \times 10^{-2} \sin(29.6x)$$

$$\bar{u}_c = 3.16 \times 10^{-2} - 1.4 \times 10^{-2} \cos(4.65x) - 1.76 \times 10^{-2} \cos(29.6x)$$



$$m_1^2 = \frac{3}{2}$$

$$k = \frac{1}{2}$$

f = 960 cps

Figure 5.- Variations of \bar{u}_r and \bar{u}_c for large frequency.

x
metres

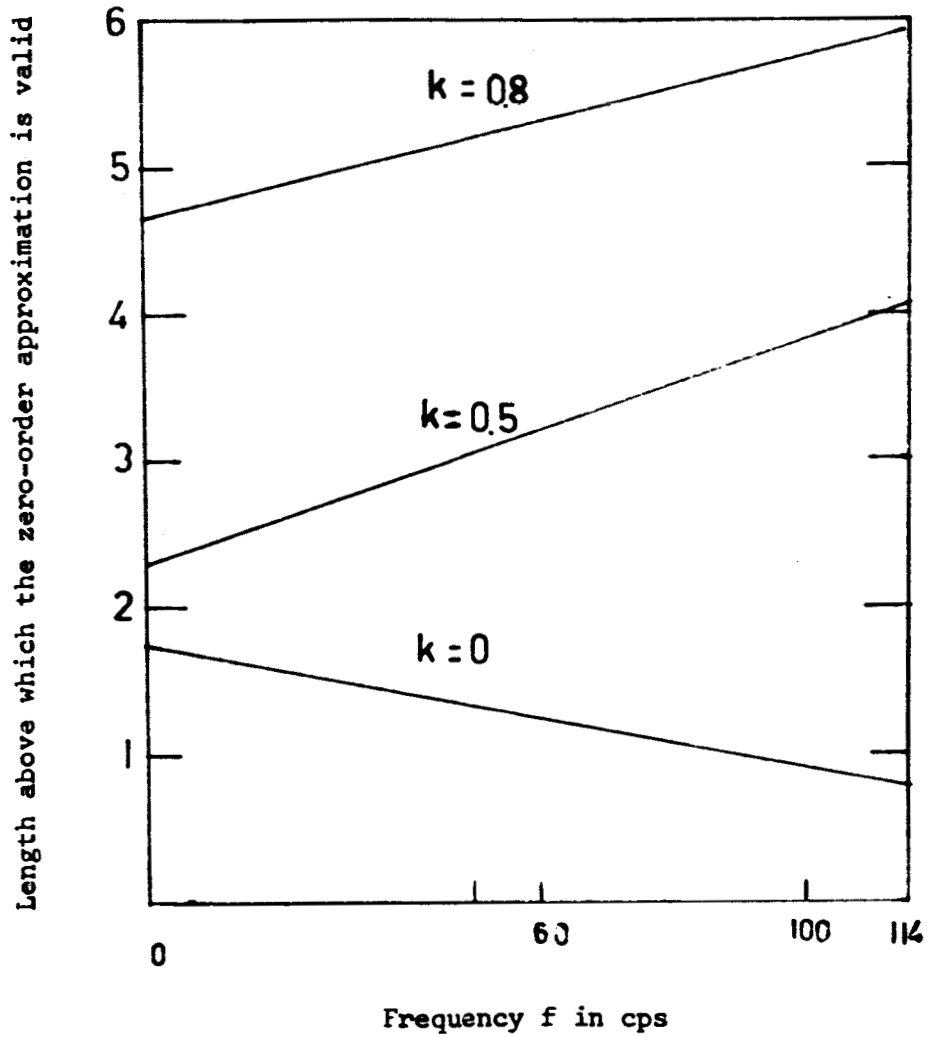


Figure 6.- Validity of the zero-order approximation.

$$\bar{u} = \bar{u}_r + j\bar{u}_c \quad \text{and} \quad \frac{u_{per}}{u_o} = \text{Re}(\bar{u} \exp(2j\omega t))$$

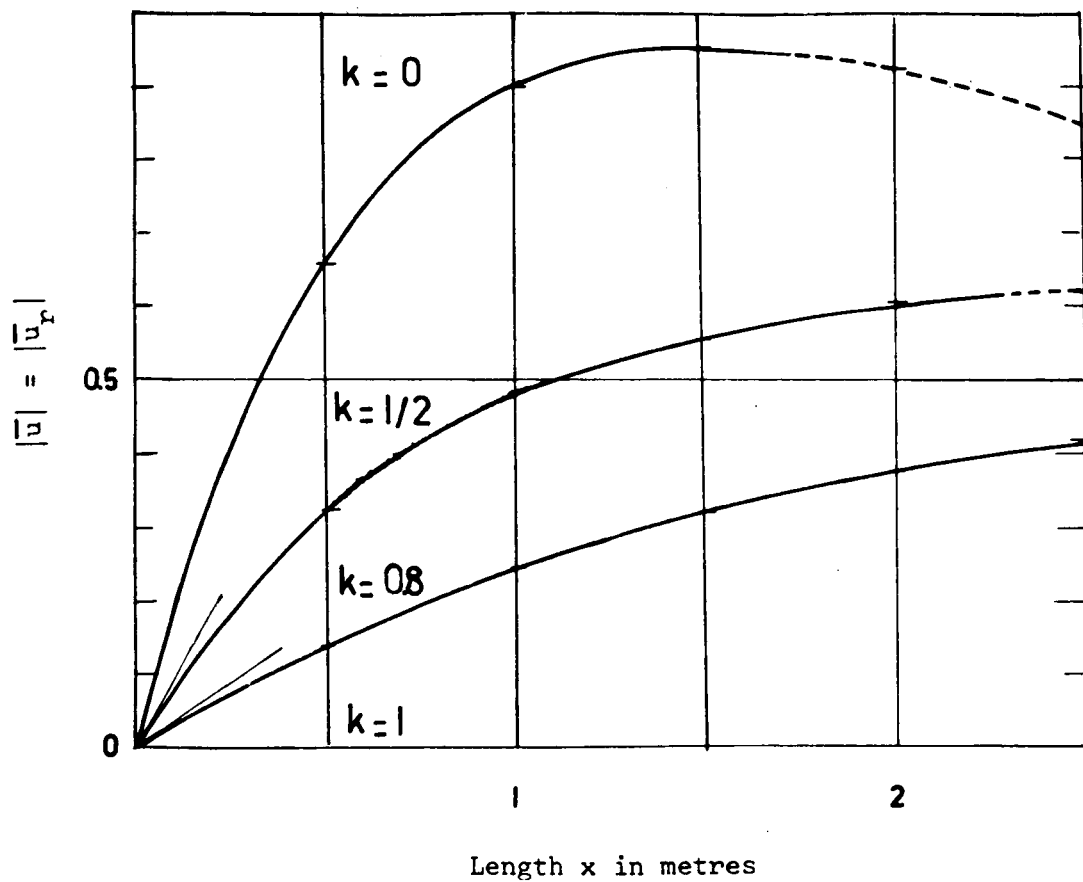
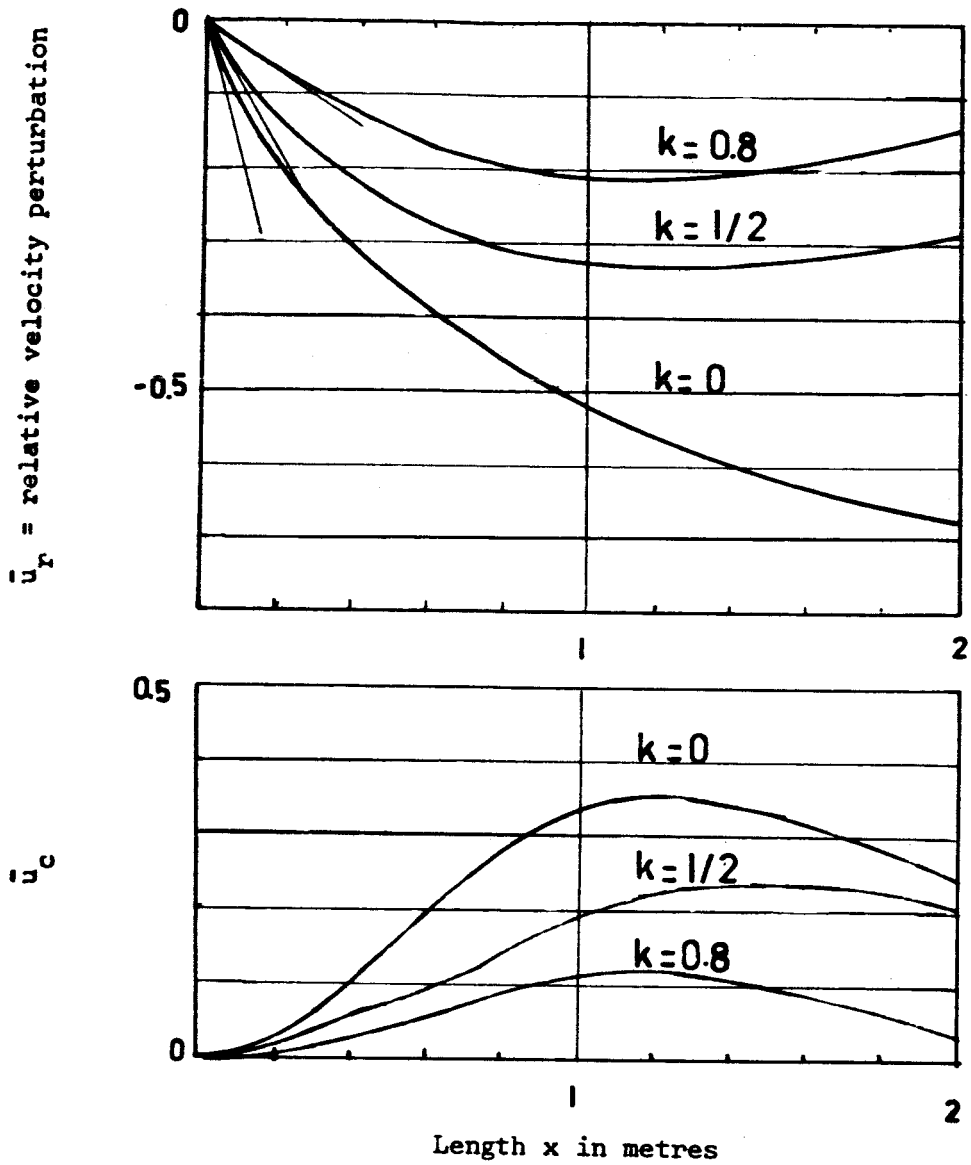


Figure 7.- Relative velocity perturbation for a d.c. self-excited generator ($f = 0$ cps).



$$\frac{u}{u_0} \text{ per} = \text{Re}(\bar{u} \exp(2j\omega t)) \quad \text{and} \quad \bar{u} = \bar{u}_r + j\bar{u}_c$$

Figure 8a.- Variation of \bar{u}_r and \bar{u}_c along the channel of an a.c. self-excited generator for a frequency $f = 28.5$ cps.

$$\bar{u} = \bar{u}_r + j\bar{u}_c$$

$$\frac{u_{per}}{u_o} = \text{Re}(\bar{u} \exp(2j\omega t))$$

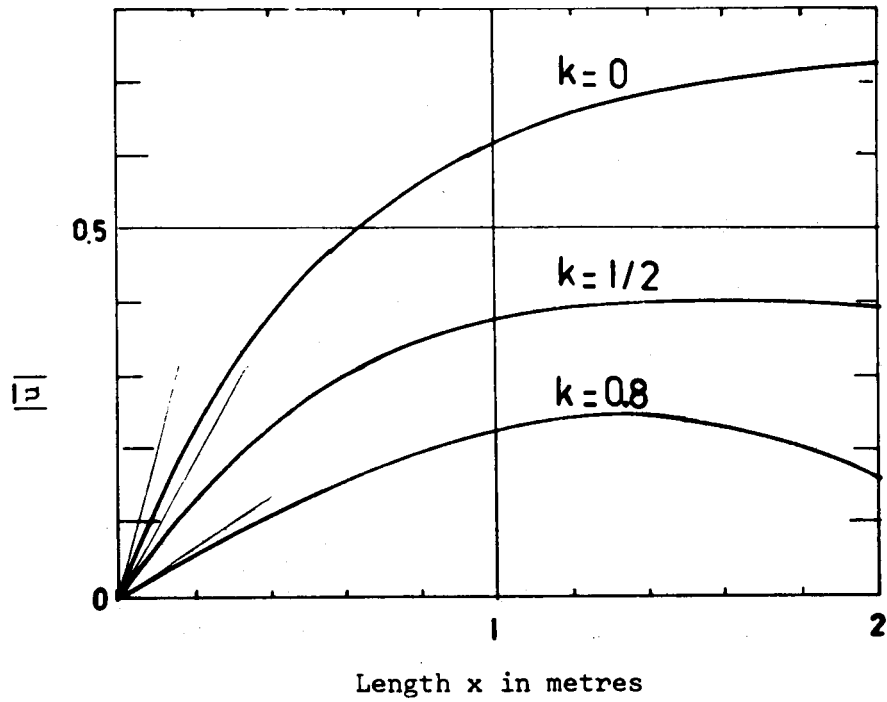


Figure 8b.- Variation of $|\bar{u}|$ along the channel of an a.c. self-excited generator for $f = 28.5$ cps.

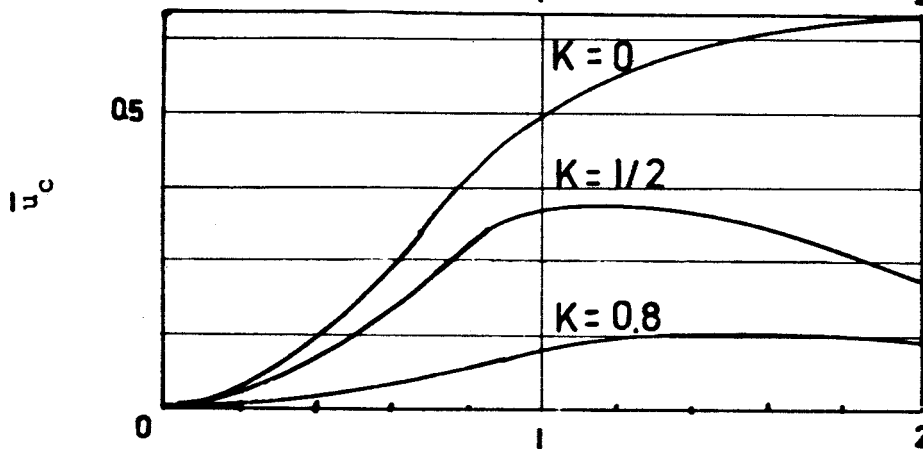
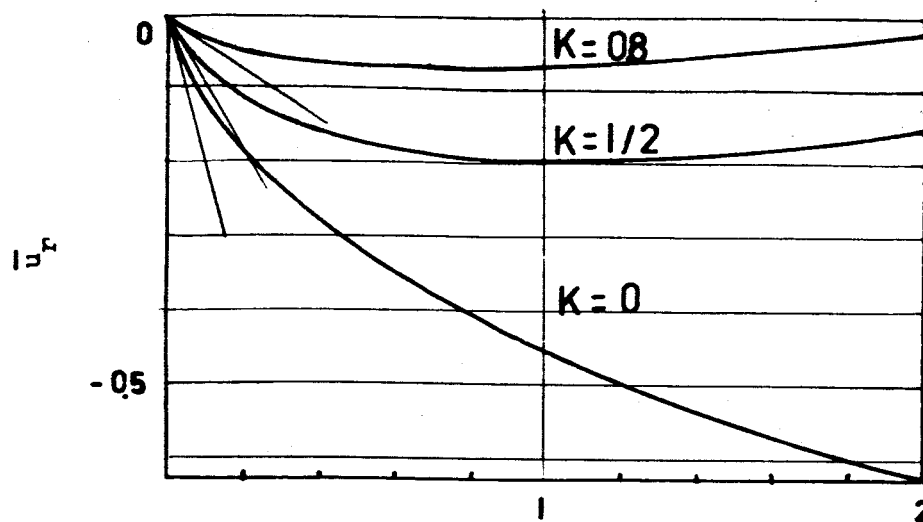


Figure 9a.- Variation of \bar{u}_r and \bar{u}_c along the channel of an a.c. self-excited generator for a frequency $f = 57$ cps.

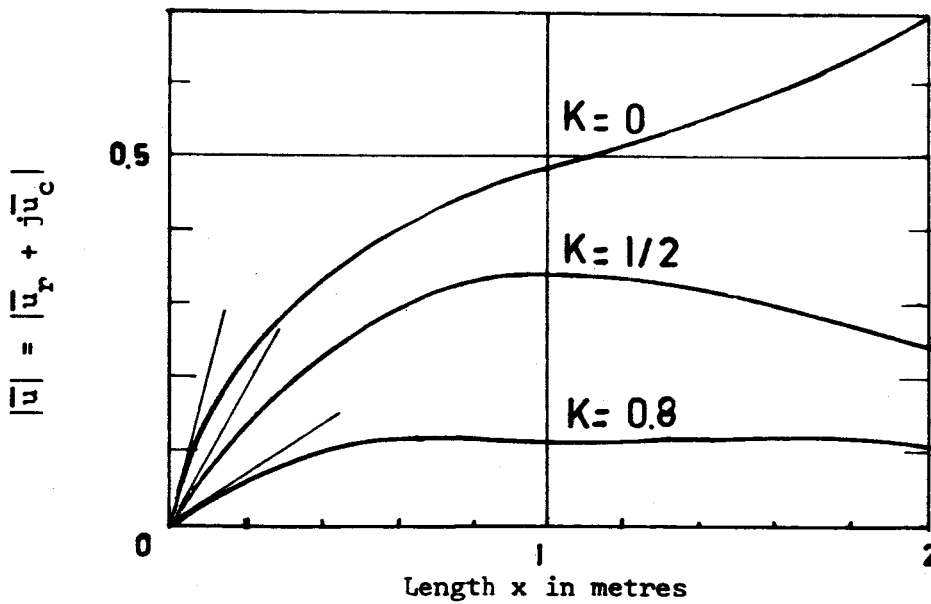


Figure 9b.- Variation of $|\bar{u}|$ along the channel of an a.c. self-excited generator for $f = 57$ cps.

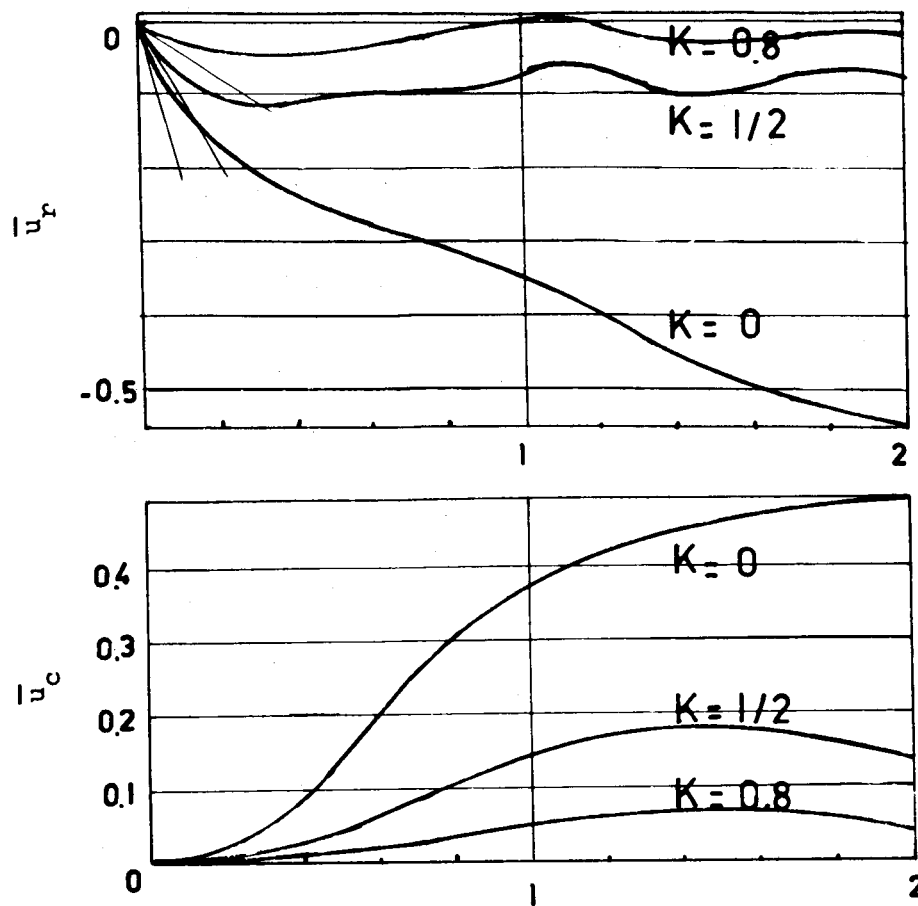


Figure 10a.- Variation of \bar{u}_r and \bar{u}_c along the channel of an a.c. self-excited generator for a frequency $f = 114$ cps.

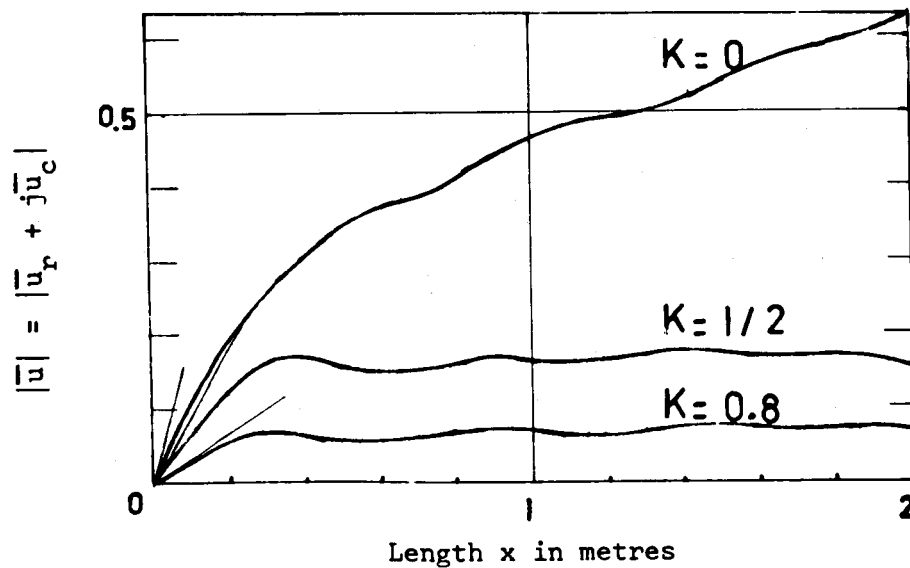


Figure 10b.- Variation of $|\bar{u}|$ along the channel of an a.c. self-excited generator for $f = 114$ cps.

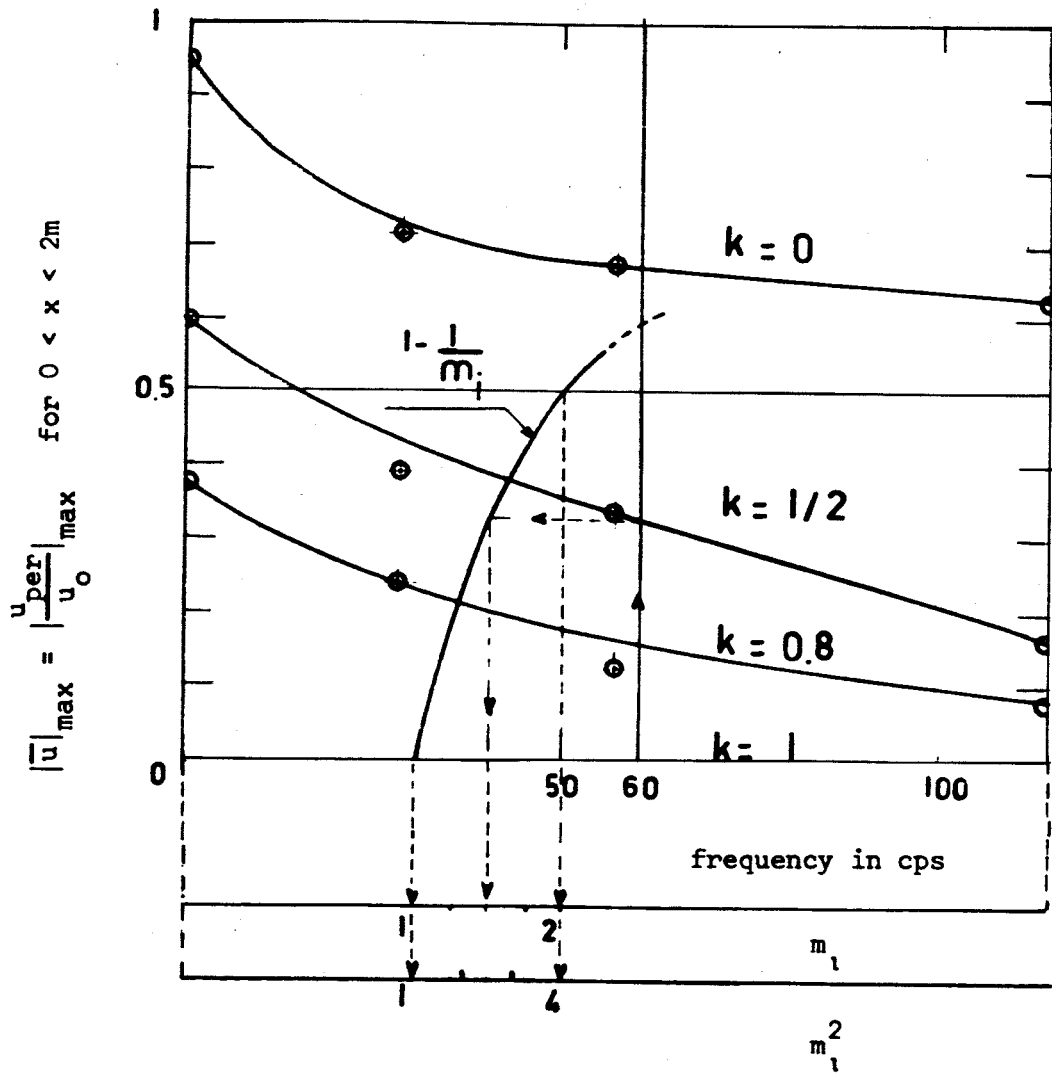


Figure 11.- Validity of the linear analysis of small perturbations (zero-order: $0 < x < 2m$).

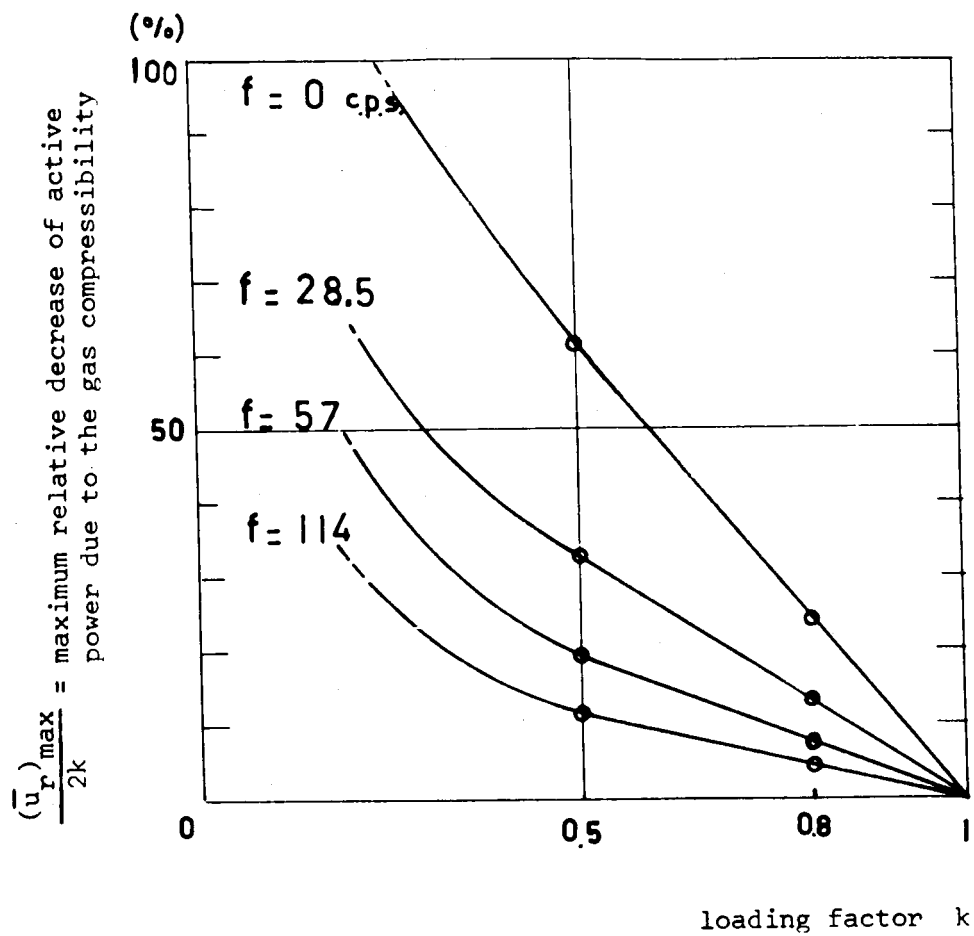


Figure 12.- Maximum relative decrease of active power density due to the gas compressibility for $0 < x < 2m$.

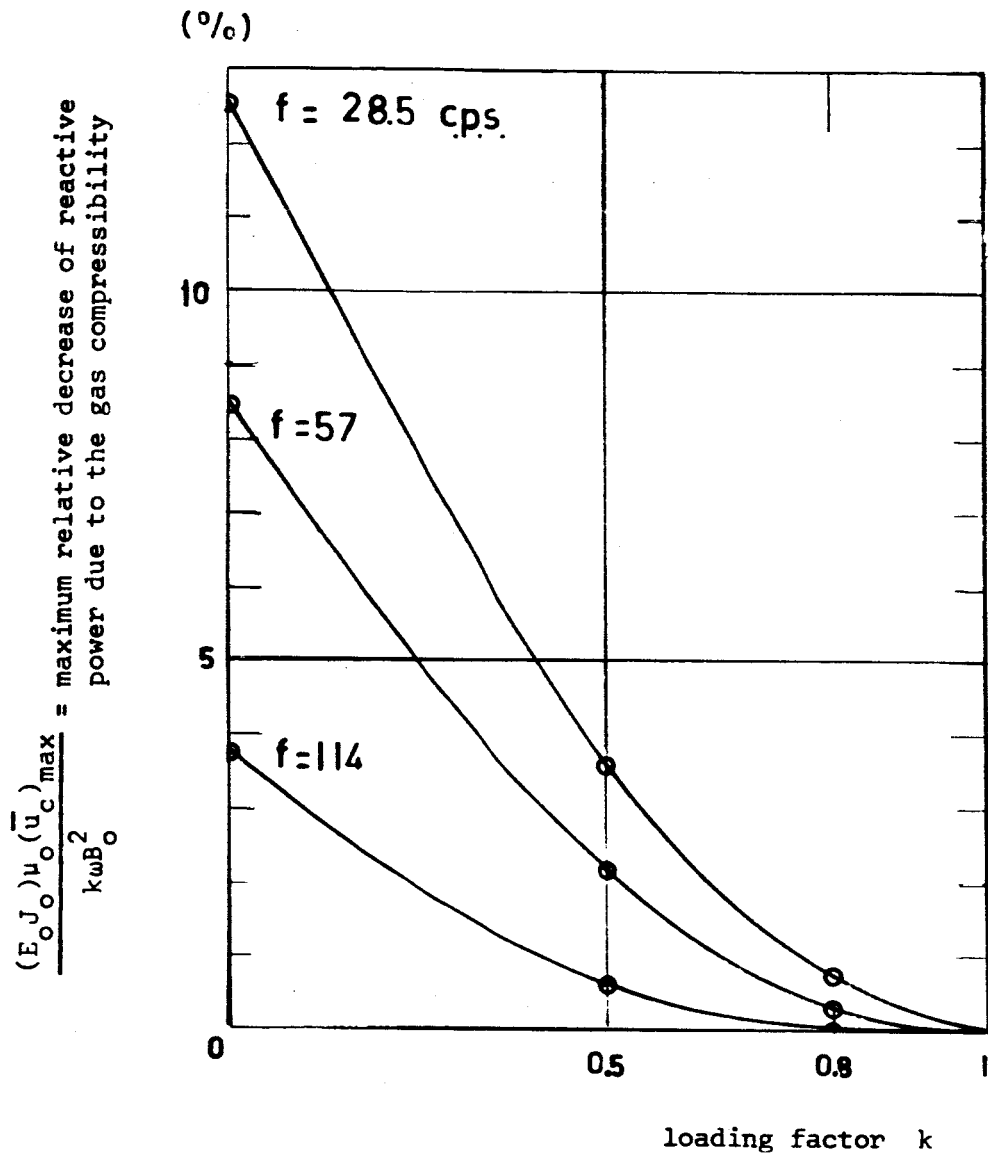


Figure 13.- Maximum relative decrease of reactive power density due to the gas compressibility for $0 < x < 2m$.